

## Article

# Effect of Zeolite Content on Permeability of Stone Chip-Bentonite-Zeolite Mixture Using a Single Solution

Sifa Xu <sup>1</sup>, Yajun Fu <sup>1</sup>, Jun Wang <sup>1</sup>, Jianwei Lv <sup>1</sup>, Xiaobing Xu <sup>1</sup> , Weiwei Wei <sup>2</sup> and Zhe Wang <sup>1,\*</sup> <sup>1</sup> Institute of Geotechnical Engineering, Zhejiang University of Technology, Hangzhou 310023, China<sup>2</sup> Zhongtian Construction Group Co., Ltd., Dongyang 322100, China

\* Correspondence: wangzsd@zjut.edu.cn

**Abstract:** Bentonite is frequently utilized as a landfill lining material due to its high impermeability. Due to the fact that heavy metal ions in leachate can alter the permeability of bentonite liner, the impermeability and metal adsorption effect of bentonite liner is typically enhanced by the use of external admixtures. In this investigation, zeolite was combined with stone chips and bentonite. Using a flexible wall permeation test, zeta potential test, and X-ray diffraction test, the effect of zeolite on the permeability and adsorption properties of the mixture was investigated. The results indicate that the addition of zeolite can enhance the impermeability of the mixed soil. The permeability coefficient of the mixed soil in DIW is  $3.74 \times 10^{-7}$  cm/s when bentonite is incorporated at 11% and decreases to  $6.55 \times 10^{-8}$ ,  $4.65 \times 10^{-8}$ , and  $5.10 \times 10^{-8}$  cm/s when 12.50%, 25%, and 50% of zeolite are incorporated; the permeability coefficient of the mixed soil in DIW was  $3.74 \times 10^{-7}$  cm/s when the permeate concentration was 0.01 mol/L of ZnCl<sub>2</sub> solution, the permeation coefficients were  $5.73 \times 10^{-7}$ ,  $5.98 \times 10^{-8}$ ,  $5.8 \times 10^{-8}$ , and  $5.7 \times 10^{-8}$  cm/s when the zeolite doping was 0, 12.50, 25, or 50%, respectively, and the Zn<sup>2+</sup> concentration of the leachate decreased compared to the no-zeolite case by 92.48, 97.29, and 98.65%, respectively; the competitive adsorption of metal ions by zeolites in ionic solutions of different concentrations reduced the ionic concentration in the solution and decreased the inhibition of bentonite swelling, while the adsorption characteristics of stone chip-bentonite-zeolite mixture on Zn<sup>2+</sup> were measured by the Langmuir and Freundlich et al. model.

**Keywords:** stone chip-bentonite-zeolite mixture; zeolite; permeation properties; ion concentration; adsorption mode



**Citation:** Xu, S.; Fu, Y.; Wang, J.; Lv, J.; Xu, X.; Wei, W.; Wang, Z. Effect of Zeolite Content on Permeability of Stone Chip-Bentonite-Zeolite Mixture Using a Single Solution. *Appl. Sci.* **2022**, *12*, 11732. <https://doi.org/10.3390/app122211732>

Academic Editor: Nikolaos Koukoulas

Received: 13 October 2022  
Accepted: 16 November 2022  
Published: 18 November 2022

**Publisher's Note:** MDPI stays neutral with regard to jurisdictional claims in published maps and institutional affiliations.



**Copyright:** © 2022 by the authors. Licensee MDPI, Basel, Switzerland. This article is an open access article distributed under the terms and conditions of the Creative Commons Attribution (CC BY) license (<https://creativecommons.org/licenses/by/4.0/>).

## 1. Introduction

In order to prevent landfill leachate from flowing into the ground and contaminating the surrounding soil, an impermeable barrier with an “anti-blocking” effect is placed at the bottom or edge of the landfill [1]. Compacted clay layers not only have high impermeability but also can prevent sharp objects, such as stones, from piercing the geomembrane to play a protective role and are used in landfill impermeability systems [2].

Bentonite can meet the impermeability requirements of liner systems because of its high swelling capacity and low permeability coefficient [3], while sand can also improve the thermal conductivity, compaction, mechanical strength, and long-term stability of engineering barriers and reduce engineering costs [4]. Therefore, bentonite-doped sand mixtures are often used instead of natural clay in areas where natural clay is scarce. Otoko et al. [5] added bentonite to sand and found that the permeability of sand-bentonite mixtures was significantly reduced from  $10^{-4}$  cm/s to large  $10^{-8}$  cm/s.

Additionally, it has been demonstrated that the nonmetallic clay material bentonite is efficient at removing heavy metal ions [6]. Montmorillonite, the main mineral in bentonite, is a 2:1 type aluminosilicate consisting of two silica-oxygen tetrahedra and a central alumina octahedral sheet [7]. The cell layer structure contains some unstable cations and is easily exchanged with other cations in solution [8]; therefore, bentonite has a high cation exchange

capacity. Through adsorption tests, Abidin et al. [9] indicated that  $Zn^{2+}$  adsorption by bentonite increases with increasing initial ion concentration. Liu et al. [10] found that the adsorption of metal ions by bentonite is affected by the solution pH; Sodium-based bentonite dosage, contact time, and temperature were found to be highly influenced. In addition, bentonite has some excellent physicochemical properties, including a large specific surface area, chemical stability, low cost, high porosity, and ubiquitous availability [11]. Based on these benefits, there is a significant amount of space for further investigation into the application of bentonite for the adsorption of heavy metal ions in landfills.

The swelling properties and permeability characteristics of bentonite are affected when it encounters heavy metal ions [12]. This is mainly due to the fact that the free swelling of bentonite gradually decreases with increasing ionic valence and concentration in solution [13], leading to a gradual increase in the permeability coefficient of bentonite. The effect of ion concentration on the permeability coefficient is the dominant factor at lower ( $\leq 0.01$  M) or higher ( $\geq 1$  M) ion concentrations [14].

In order to reduce the influence of heavy metal ions on the permeability of bentonite, the influence of heavy metals on the swelling properties of bentonite is generally reduced by the addition of adsorbents, and zeolite is one of the more commonly used additives [15]. Barakat [16] found experimentally that the adsorption capacity of zeolites for metal ions strongly depends on the initial metal ion concentration. Iskander et al. [17] found that both natural zeolite and bentonite have better adsorption properties for metal  $Zn^{2+}$  in controlled tests. Salem et al. [18] showed by the results that the addition of 66.67%, 29.17%, and 4.16 wt.% zeolite, bentonite, and kaolin, respectively, can optimize the adsorption capacity of the mixture for metal ions simultaneously.

Stone chips are an excellent material for sand even though, in addition to sharing many of the same fundamental physical properties as natural sand, the resources of stone chips in China are extremely abundant. Therefore, the use of stone chips as a potential substitute for river sand in sand-bentonite mixtures, the formation of stone chips-bentonite-zeolite as new impermeable materials, and the transformation of stone chips into a treasure through comprehensive use are all methods where these materials can assist in saving resources.

In this study, zeolite was combined with stone chips and bentonite to study the permeability of the soil mixture and investigate the possibility of using stone chips in the location of sand.  $Zn^{2+}$  was selected as the ionic solution to evaluate the new material's adsorption capability and to establish a microscopic mechanism to explain it.

## 2. Materials and Methods

### 2.1. Materials

#### (1) Bentonite

The test bentonite was produced in Anji County, Zhejiang Province, with the appearance of off-white powder. An X-ray diffractometer (XRD) test analysis showed that the bentonite was sodium-based bentonite, whose main components consisted of montmorillonite (78.50 wt.%), quartz (78.50 wt.%), and feldspar (5.60 wt.%), as shown in Figure 1. It had a relative density of 2.72, a liquid limit of 218%, a plastic limit of 43%, a plasticity index of 175, a total cation-exchange capacity of 0.77 meq/g, and a swelling capacity of 8.50 mL/g in deionized water (DIW).

#### (2) Zeolite

The test zeolite was produced from a water purification plant in Henan Province and was a grayish-white silicate mineral with a microporous structure and solid adsorption and ion exchange capacity. The silica-oxygen tetrahedron is the most fundamental building block of the zeolite framework. From XRD analyses, it has been shown that the primary zeolite constituents are  $SiO_2$  (63.90%),  $Al_2O_3$  (13.60%), CaO (2.80%), MgO (2.40%),  $Fe_2O_3$  (1.30%), and  $K_2O$  (2.80%). Loss-on-ignition for the zeolite was 12.83%.

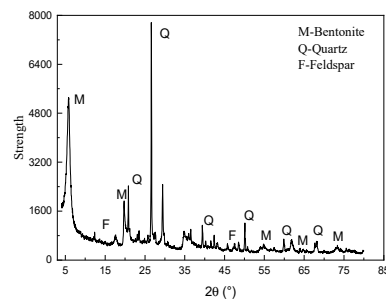


**Figure 1.** XRD diffraction diagram of bentonite.

### (3) Stone chips

As shown in Figure 2, the stone chips, which formed the matrix of the soil mixture, were obtained from a quarry in Anji County, Zhejiang Province, with a maximum particle size of 5 mm, an acceptable particle content of 7.48%, a uniformity coefficient  $C_u$  of 11.78, and a curvature coefficient  $C_c$  of 1.06. The resulting soil mixture had a satisfactory aggregate grade. According to the geotechnical experimental specification standard, we used the compaction test to obtain the optimum moisture content of the specimen of 7.50% and the maximum dry density of  $1.99 \text{ g/cm}^3$ . Through the sieving experiment, we obtained the gradation parameters of stone chips with  $d_{50} = 1.10 \text{ mm}$ ,  $C_u = 13.27$ , and  $C_c = 1.82$ , which indicated that the experimental stone chips were well-graded. The variable head infiltration test showed that the average permeability coefficient of the stone chips was  $1.76 \times 10^{-4} \text{ cm/s}$  at 100% compaction. The stone chips did not meet the permeability requirements of the landfill liner system, i.e.,  $1 \times 10^{-7} \text{ cm/s}$ .



**Figure 2.** The appearance of stone chips.

## 2.2. Experimental Procedures

The test scheme consisted of three parts. Part 1 involved investigating the effects of the zeolite content and contaminant concentration on the swelling properties of the bentonite at different  $\text{ZnCl}_2$  concentrations (0, 0.01, 0.03, 0.05, 0.10, and 1.00 mol/L). Part 2 investigated the impacts of zeolite content on the permeability performance of a soil mixture (made with bentonite–stone chip mass ratio of 11%) at various  $\text{ZnCl}_2$  concentrations (0, 0.01, 0.03, and 0.10 mol/L). The  $\text{Zn}^{2+}$  concentration of the leachate at the end of the permeability tests was measured. Referring to the scheme of bentonite and zeolite adsorption tests on  $\text{Zn}^{2+}$  in the relevant literature [19,20], we determined the concentration of  $\text{Zn}^{2+}$  ions for the adsorption tests in this study. Part 3 investigated the adsorption characteristics of mixed soils with different zeolite doping (0, 12.50, 25, and 50%) for different concentrations of  $\text{Zn}^{2+}$  ions (0, 3, 5, 10, 20, 30, and 50 mmol/L) by batch adsorption tests, allowing isothermal adsorption in static equilibrium at the soil to water ratio of 1:20. The test soil to water ratio was determined by referring to the  $\text{Zn}^{2+}$  [21,22] adsorption test with bentonite and zeolite alone as adsorbent materials. Electric potential analysis was conducted after adsorption to explain the relationship between the adsorption capacity and the electric double layer. All tests were conducted at  $25 \text{ }^\circ\text{C}$ .

### 2.3. Test Methods and Apparatus

Soil-mixture specimens with a 7.50% water content and different zeolite contents were prepared by mixing the zeolite, bentonite, stone chips, and DIW. The mixture was stirred evenly and allowed to settle for 24 h. The mixture for each specimen was divided into five equally weighted parts that were separately filled into a mold (70 mm in diameter and 140 mm high) and compacted layer by layer using a compactor, with a compaction process using standard light compaction instrument, a 2.5 kg hammer weight, a hammer bottom diameter of 51 mm, drop distance of 305 mm, and unit body compaction work of about 592.20 KJ/m<sup>3</sup>. The resulting soil column was vacuum-impregnated with compaction of 100% and a dry density of 1.99 g/cm<sup>3</sup> based on the liquid-plastic limit and compaction tests. The synthesized heavy metal-containing aqueous solution is made using the selected heavy metal (Zn<sup>2+</sup>). All solutions were made up of deionized water and diluted according to the desired concentrations.

As shown in Figure 3a, permeability tests were conducted using a fully automatic soil permeability tester (GDS, UK), which mainly consisted of a pressure cell, a volume controller, and an air-pressure system. GDS uses the principle of normal head infiltration test to calculate the infiltration velocity and hydraulic gradient by measuring the seepage volume, the head height at different points, and thus the infiltration coefficient by substituting into Equation (1):

$$k = \frac{VL}{A\Delta ht} \quad (1)$$

where  $\Delta h$  is the poor water head (m),  $k$  is the coefficient of permeability (cm/s),  $A$  is the water flowing through the cross-sectional area (cm<sup>2</sup>),  $V$  is the amount of water flowing through the specimen after  $t$  time (cm<sup>3</sup>),  $L$  is the length of saturated specimen (cm), and  $t$  is the test duration(s).

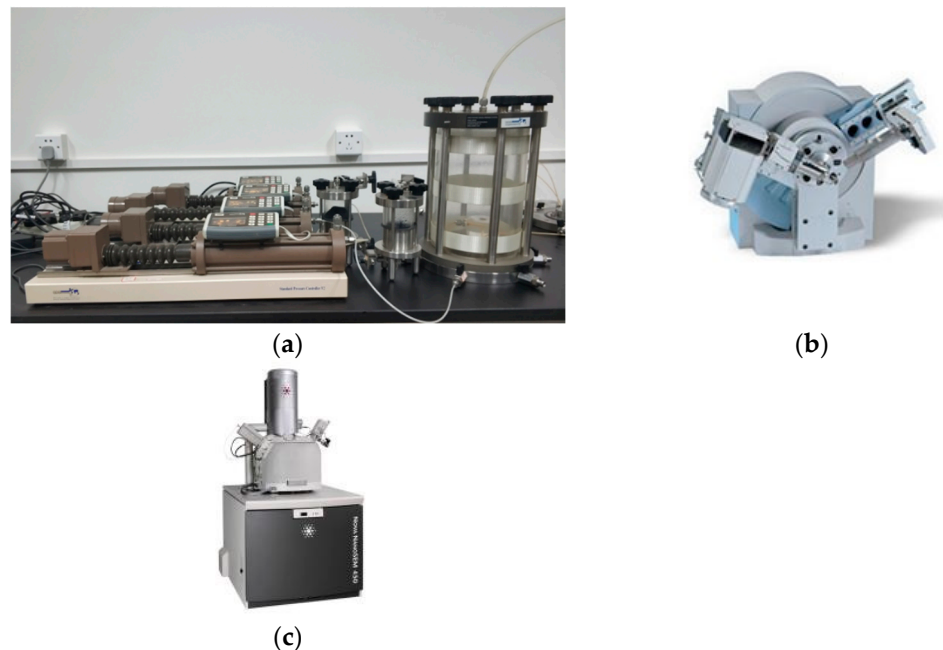


**Figure 3.** Permeation experiment-related instruments. (a) GDS; (b) XRD; (c) SEM.

The principle of instrumental determination of the permeability coefficient of mixed soil is based on a variable head experiment. The water pressures upstream and downstream of the adsorbent were controlled through the pressure-volume controller. The confining pressure was applied using the air-pressure system. The permeability coefficient measurement range was 10<sup>-5</sup>–10<sup>-9</sup> cm/s. The volume controller and air-pressure system had a pressure-configuration range of 0–1 MPa. Permeability tests were conducted at a confining pressure of 300 kPa, upstream water pressure of 200 kPa, and downstream water pressure

of 100 kPa; the leachate was simulated using  $\text{ZnCl}_2$  solutions of different concentrations (DIW, 0.01, 0.03, and 0.10 mol/L).

In order to investigate the changes in the permeability coefficient of mixed soil from a microscopic point of view, we applied the X-ray diffraction (XRD) technique and the scanning electron microscope (SEM) technique to examine the mixed soil at the end of the permeability experiment. The XRD device was used to test the mineral composition of bentonite and zeolite with the radiation, as shown in Figure 3b. The surface morphology of bentonite after the adsorption experiment was characterized using the SEM (Zeiss Sigma 300) operated at an accelerating voltage of 5 kV to examine and analyze the surface morphology and provide evidence of the effects of heavy metal cations after adsorption, as shown in Figure 3c.

Sorption of  $\text{Zn}^{2+}$  cations was performed using the batch experiment technique of single solute reactions. The experiments were performed in 100 mL glass columns with stoppers containing ionic solution aqueous solutions of  $\text{Zn}^{2+}$  with 1 stone chip-bentonite-zeolite mixture. The adsorbent and aqueous solution were shaken at 200 rpm to reach equilibrium concentration, while the columns were kept sealed to minimize losses to the atmosphere. Samples were given a reaction time of 24 h at  $25 \pm 2$  °C, and after the reaction time, the endpoint sample was collected and filtered through a 0.20  $\mu\text{m}$  membrane filter and analyzed for heavy metal ions by AA-6300. The Japanese atomic absorption spectrophotometer (AA-6300) was used to determine the residual metal ion concentration after adsorption, as shown in Figure 4a.

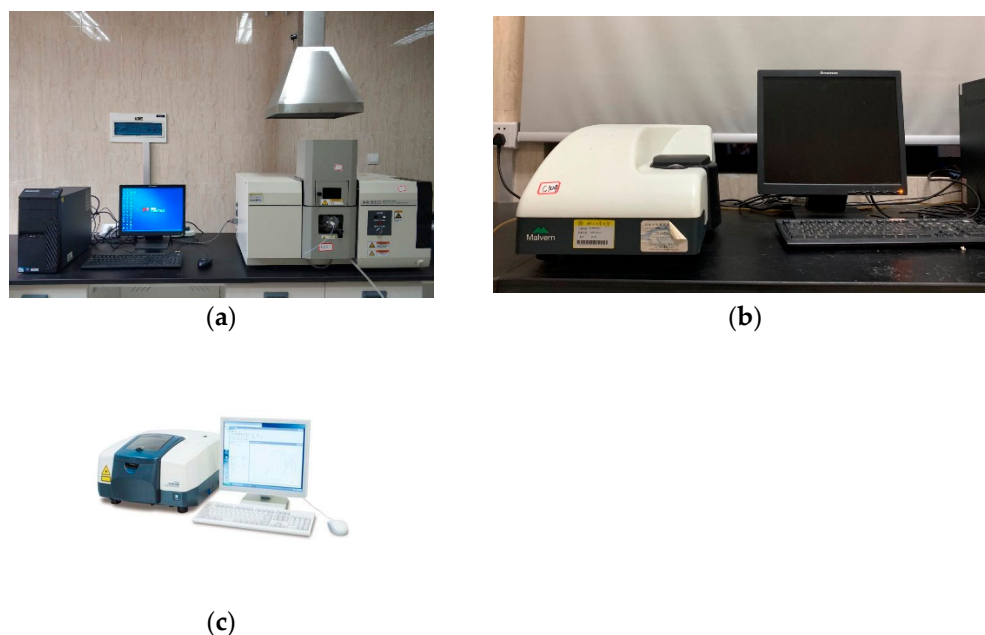


**Figure 4.** Adsorption experiment-related instruments. (a) Atomic absorption spectrometer; (b) Nanoparticle size potential meter; (c) FTIR.

In order to investigate the adsorption experiments of the mixed soil from the micro-mechanism, we did the following tests. After adsorption, 10 mL of the solution was transferred to a 250 mL volumetric flask and diluted with ultrapure water. One milliliter of the solution was injected into the cuvette (to ensure that there were no air bubbles in the cuvette), and then the cuvette was placed in the nanoparticle size potentiostat to measure the zeta potential. The stability of the particle dispersion increases with increasing absolute zeta potential, and vice versa, the more agglomeration or coagulation of particles takes place. The zeta potential was measured using a ZS90 nanoparticle size analyzer (Malvern, UK), as shown in Figure 4b. The surface functional groups of bentonite and zeolite were characterized by Fourier transform infrared spectroscopy (FTIR), as shown in Figure 4c. The IR wavelength was run between 4000 and 500  $\text{cm}^{-1}$  operating at a peak resolution of

$4 \text{ cm}^{-1}$ . The test uses the instrument model for Thermo Fisher IN10.3. The stability of particle dispersion increases with increasing absolute zeta potential and vice versa, increasing the likelihood of particle agglomeration or coagulation. The zeta potential was measured using a ZS90 nanoparticle size analyzer (Malvern, UK). Particle size, zeta potential, and molecular weight are indeed the three significant characteristics that this analyzer is made to measure in materials like colloids and polymers. It can precisely measure the zeta potential and molecular weight of both aqueous-dispersion and non-aqueous-dispersion systems and has a particle-size measurement range of 0.30–100 nm.

#### 2.4. Adsorption Kinetics

The adsorption-removal rate  $RP$  (%) and the unit adsorption capacity  $q_e$  of a soil mixture (mg/g) concerning the heavy metal  $\text{Zn}^{2+}$  are computed using Equations (2) and (3), respectively:

$$RP = \frac{C_0 - C_e}{C_0} \times 100\% \quad (2)$$

$$q_e = \frac{C_0 - C_s}{m_s} V \quad (3)$$

where  $C_0$  is the initial contaminant concentration (mg/L),  $C_e$  is the equilibrium concentration (mg/L),  $m_s$  is the adsorbent mass (g), and  $V$  is the solution volume (mL).

The adsorption capacity  $q_t$  (mg/g) concerning heavy metal  $\text{Zn}^{2+}$  at time  $t$  is expressed as:

$$q_t = \frac{C_0 - C_t}{m_s} V \quad (4)$$

where  $C_t$  is the  $\text{Zn}^{2+}$  concentration (mg/L) of the centrifuged supernatant at time  $t$ .

Four equations, the Langmuir model, the Freundlich model, the D-R isothermal adsorption model, and the Henry model, are frequently utilized to describe the isothermal adsorption of metal ions in solution by solid adsorbents. The model calculation common is shown below.

##### ① Langmuir model:

The model assumes isotropic adsorbent surface and monolayer adsorption with homogeneous adsorption. The model is usually applied to the whole isothermal adsorption process and can reflect the amount of soil adsorbed.

$$\frac{c_e}{q_e} = \frac{1}{K_L q_m} + \frac{c_e}{q_m} \quad (5)$$

where  $K_L$  is the Langmuir isotherm parameter (L/mg), and  $q_m$  is the maximum adsorption capacity (mg/g).

##### ② Freundlich model

The model assumes that the adsorbent is anisotropic and multilayered for the low-concentration phase of isothermal adsorption.

$$q_e = K_F C_e^{\frac{1}{n}} \quad (6)$$

where  $K_F$  is the adsorption capacity-related constant (L/g), and  $n$  is an empirical constant, usually greater than 1. A value greater than 1 indicates a predominantly physical adsorption process, and a larger value corresponds to a more nonlinear adsorption model.

##### ③ D-R isothermal adsorption model

The model assumes that the adsorbed solute fills in the pores

$$\ln q_e = \ln q_m - k\varepsilon^2 \quad (7)$$

$$\varepsilon = RT \ln \left( 1 + \frac{1}{c_e} \right) \quad (8)$$

$$E = -\frac{1}{\sqrt{2k}} \quad (9)$$

where,  $k$  correlation model constant ( $\text{mol}^2 \cdot \text{kJ}^{-2}$ ), maximum adsorption ( $\text{mol} \cdot \text{g}^{-1}$ ),  $\varepsilon$  is the Polanyi potential, which is related to the equilibrium concentration ( $\text{kJ} \cdot \text{L} \cdot \text{mol}^{-2}$ ),  $R$  ideal other constants,  $T$  thermodynamic temperature (K),  $E$  average free energy of adsorption ( $\text{kJ} \cdot \text{mol}^{-1}$ )

④ Henry model

$$q_e = k_d C_e \quad (10)$$

### 3. Results and Discussion

#### 3.1. Effect of Zeolite Content on Swelling Characteristics of Bentonite

Figure 5 shows zeolite–bentonite mixture specimens with different zeolite-to-bentonite mass ratios (12.50, 25, and 50%) were prepared using 2 g of bentonite as the basic dilator. The specimens were subjected to free-swelling tests in DIW and  $\text{ZnCl}_2$  solutions of different concentrations. It was investigated that the zeolite content and the swelling capacity of the bentonite were related. Zeolite–bentonite mixture specimens with different zeolite-to-bentonite mass ratios (12.50, 25, and 50%) were prepared using 2 g of bentonite as the basic dilator. The specimens were subjected to free-swelling tests in DIW and  $\text{ZnCl}_2$  solutions of different concentrations. It could be indicated that the zeolite content and the swelling capacity of the bentonite were related.

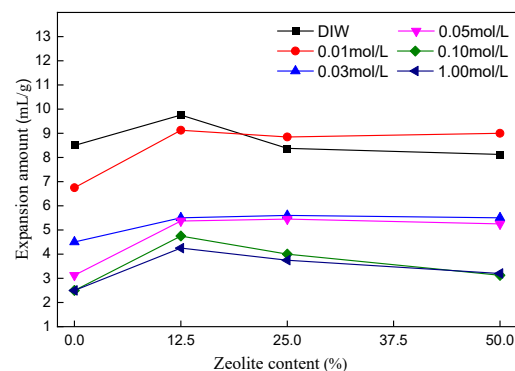


**Figure 5.** Variation of the swelling volume of mixed soil with different zeolite admixtures.

When in contact with DIW, pure bentonite had a maximum swelling capacity of 8.50 mL/g. The specimens with zeolite contents of 12.50, 25, and 50% had swelling capacities of 9.75, 8.38, and 8.13 mL/g, respectively, indicating that overall, the addition of zeolite had an insignificant effect on the swelling characteristics of the bentonite. When in contact with the  $\text{ZnCl}_2$  solution, the swelling capacity of pure bentonite decreased with increasing contaminant concentration. The swelling capacities at  $\text{ZnCl}_2$  concentrations of 0.01, 0.03, 0.05, 0.1, and 1.0 mol/L were 6.75, 4.50, 3.13, 2.50, and 2.50 mL/g, respectively; the swelling capacity of the pure bentonite at the  $\text{ZnCl}_2$  concentration of 1.00 mol/L was 3.40 times lower than that of the pure bentonite in contact with DIW. The specimen with 12.50% zeolite content had swelling capacities of 9.13, 5.50, 5.38, 4.75, and 4.25 mL/g for contaminant concentrations of 6.75, 4.50, 3.13, 2.50, and 2.50 mL/g, respectively. These values were higher than those for pure bentonite by 2.38, 1.00, 2.25, 2.25, and 1.75 mL/g, respectively, indicating that adding the zeolite improved the swelling. At low contaminant concentrations, increasing the zeolite content from 12.50 to 25 and 50% did not change the swelling capacity significantly.

### 3.2. Effect of Ion Concentration on the Permeability of Soil Mixtures

Experimental results show the permeability coefficients of the bentonite–stone chip mixture at a degree of compactness of 100% and at different bentonite contents when in contact with DIW. The permeability coefficient of the soil mixture decreased as the bentonite content increased. The soil mixture had permeability coefficients of  $7.99 \times 10^{-5}$ ,  $3.03 \times 10^{-5}$ ,  $9.80 \times 10^{-7}$ ,  $3.74 \times 10^{-7}$ , and  $2.50 \times 10^{-7}$  cm/s for bentonite contents of 5, 7, 9, 11, and 13%, respectively. When the bentonite content increased to 9%, the permeability coefficient decreased to  $10^{-7}$  cm/s, which is the level required for anti-seepage applications.

Figure 6 shows the permeability coefficients of the zeolite–bentonite–stone chip mixture for a bentonite content of 11% and different zeolite contents and  $\text{ZnCl}_2$  concentrations. The pure bentonite–stone chip mixture had a permeability coefficient of  $3.74 \times 10^{-7}$  cm/s when in contact with DIW. Adding 12.50% zeolite reduced the permeability coefficient to  $6.55 \times 10^{-8}$  cm/s. As the zeolite content increased to 25 and 50%, the permeability coefficient decreased to  $4.65 \times 10^{-8}$  and  $5.1 \times 10^{-8}$  cm/s, respectively. This finding indicates that adding zeolite improves the anti-seepage performance of the soil mixture when in contact with pure water. At a  $\text{ZnCl}_2$  concentration of 0.01 mol/L, the bentonite–stone chip mixture (0% zeolite content) had a permeability coefficient of  $5.73 \times 10^{-7}$  cm/s. Adding 12.50, 25, and 50% zeolite increased the permeability coefficient to  $5.98 \times 10^{-8}$ ,  $5.80 \times 10^{-8}$ , and  $5.70 \times 10^{-8}$  cm/s, respectively. For zeolite contents of 0, 12.50, 25, and 50%, the soil mixture had permeability coefficients of  $9.30 \times 10^{-6}$ ,  $4.43 \times 10^{-6}$ ,  $6.59 \times 10^{-6}$ , and  $2.60 \times 10^{-6}$  cm/s, respectively, for 0.03 mol/L  $\text{ZnCl}_2$ , and  $1.40 \times 10^{-5}$ ,  $7.9 \times 10^{-6}$ ,  $3.27 \times 10^{-6}$ , and  $1.28 \times 10^{-6}$  cm/s at 0.10 mol/L  $\text{ZnCl}_2$ . The permeability coefficients exceeded  $1.0 \times 10^{-7}$  cm/s, which is required for anti-seepage liners.

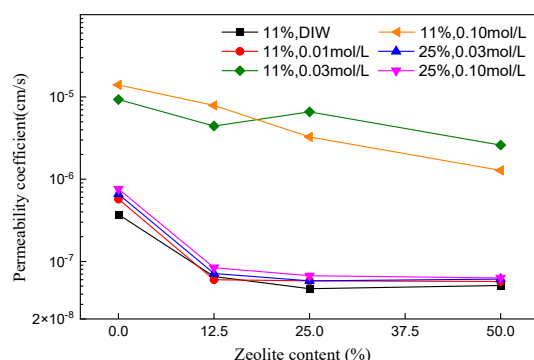


**Figure 6.** Effect of simultaneous variation of  $\text{ZnCl}_2$  concentration and zeolite admixture on the permeability coefficient of mixed soils.

For a bentonite content of 25%, the zeolite–bentonite–stone chip mixture had permeability coefficients of  $6.60 \times 10^{-7}$ ,  $7.13 \times 10^{-8}$ ,  $5.80 \times 10^{-8}$ , and  $6.10 \times 10^{-8}$  cm/s at the zeolite contents of 0, 12.50, 25, and 50% when in contact with the 0.03 mol/L  $\text{ZnCl}_2$  solution and  $7.60 \times 10^{-7}$ ,  $8.40 \times 10^{-8}$ ,  $6.70 \times 10^{-8}$ , and  $6.30 \times 10^{-8}$  cm/s when in contact with the 0.10 mol/L  $\text{ZnCl}_2$  solutions, respectively. Overall, the addition of zeolite reduced the permeability coefficient of the soil mixture to the  $1 \times 10^{-8}$  cm/s level, causing an average decrease of one order of magnitude. These results indicate that when in contact with a  $\text{ZnCl}_2$  solution with a concentration greater than 0.03 mol/L, the bentonite content of the soil mixture must be increased to 25% to satisfy the requirements for anti-seepage applications. It can be seen that the addition of zeolite can effectively reduce the permeability coefficient of the mixture. The addition of zeolite in DIW can fill the voids between the particles of the mixture, thus increasing the water seepage path and enhancing the impermeability of the mixed soil. In different concentrations of an ionic solution, the competitive adsorption of metal ions by zeolite shares the contraction pressure of the double bentonite layer, maintains the original pore structure, does not appear to have a significant seepage channel, and improves the chemical compatibility of the mixed soil.

### 3.3. Changes in Ion Concentration of Leachate

At the end of the permeability test conducted on a soil mixture specimen with 11% bentonite content, the ionic concentration of the leachate that penetrated the soil column specimen was measured. Figure 7 shows the variation of ion concentration of the leachate with zeolite content and  $\text{ZnCl}_2$  concentration. The initial  $\text{Zn}^{2+}$  concentration of the 0.01 mol/L  $\text{ZnCl}_2$  solution was 654 mg/L at 0% ion in zeolite content, while the  $\text{Zn}^{2+}$  concentration of the leachate after the test was 42.30 mg/L. The  $\text{Zn}^{2+}$  concentration of the leachate was further reduced to 3.18, 1.14 or 0.57 mg/L after adding 12.50, 25, or 50% zeolite, respectively. The  $\text{Zn}^{2+}$  concentrations decreased by 92.48, 97.29, and 98.65%, respectively, compared to the case without zeolite, which indicated that the increase of zeolite addition significantly increased the  $\text{Zn}^{2+}$  adsorption capacity of the mixed soil, and the 50% zeolite doping had the best adsorption effect.

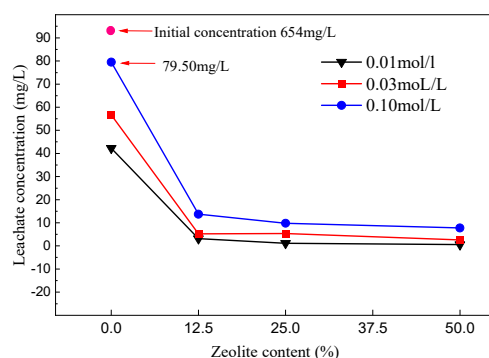


**Figure 7.** Effect of simultaneous variation of  $\text{ZnCl}_2$  concentration stone chip–bentonite–zeolite mixture zeolite admixture on leachate ion concentration.

### 3.4. Effect of Zeolite Content on Adsorption Performance of Soil Mixtures

#### (1) Ion removal rate

The relationship between the adsorption and removal rate of Zn by 15% zeolite coping stone chip-bentonite-zeolite mixture and the adsorption time under different concentration conditions are shown in Figure 8a. The adsorption and removal rates of  $\text{Zn}^{2+}$  by mixed soil were 63.49, 73.06, 80.29, 89.64, 94.89, and 95.23% at 0.25, 0.50, 1, 2, 6, and 24 h for the initial concentration of the solution of 10 mmol/L and 30 mmol/L, respectively, versus 45.93, 57.17, 67.18, 75.15, 83.01, and 83.22%. It can be seen from the graph that the removal rate of  $\text{Zn}^{2+}$  adsorption by the mixed soil became larger with the increase of time and tended to be stable after about 6 h. After 24 h of adsorption, the adsorption and removal rate of  $\text{Zn}^{2+}$  by the mixed soil remained the same with time, and it can be considered that the adsorption equilibrium was reached at this time. Therefore, the 24 h adsorption was selected as the equilibrium time for further experiment.

Figure 8b shows the variations in the  $\text{Zn}^{2+}$  adsorption-removal rate with the initial  $\text{Zn}^{2+}$  concentration. For a given initial  $\text{Zn}^{2+}$  concentration, this rate increases with increasing zeolite content. For example, for an initial  $\text{Zn}^{2+}$  concentration of 30 mmol/L, the adsorption-removal rates for zeolite contents of 0, 12.50, 25, and 50% were 67.21, 73.98, 76.01, and 83.40%, respectively. In addition, as the initial Zn concentration increased, an increase in the zeolite content produced a more notable increase in the  $\text{Zn}^{2+}$  adsorption-removal efficiency. As the initial contaminant concentration increased, the  $\text{Zn}^{2+}$  adsorption-removal rate of the soil mixture tended to decrease overall. For example, the adsorption-removal rates for zeolite contents of 0, 12.50, 25, and 50% were 98.60, 99.00, 99.07, and 99.16%, respectively, for an initial contaminant concentration of 3 mmol/L. However, these values decreased to 62.58, 68.50, 73.31, and 78.18%, respectively, for an initial contaminant concentration of 50 mmol/L.

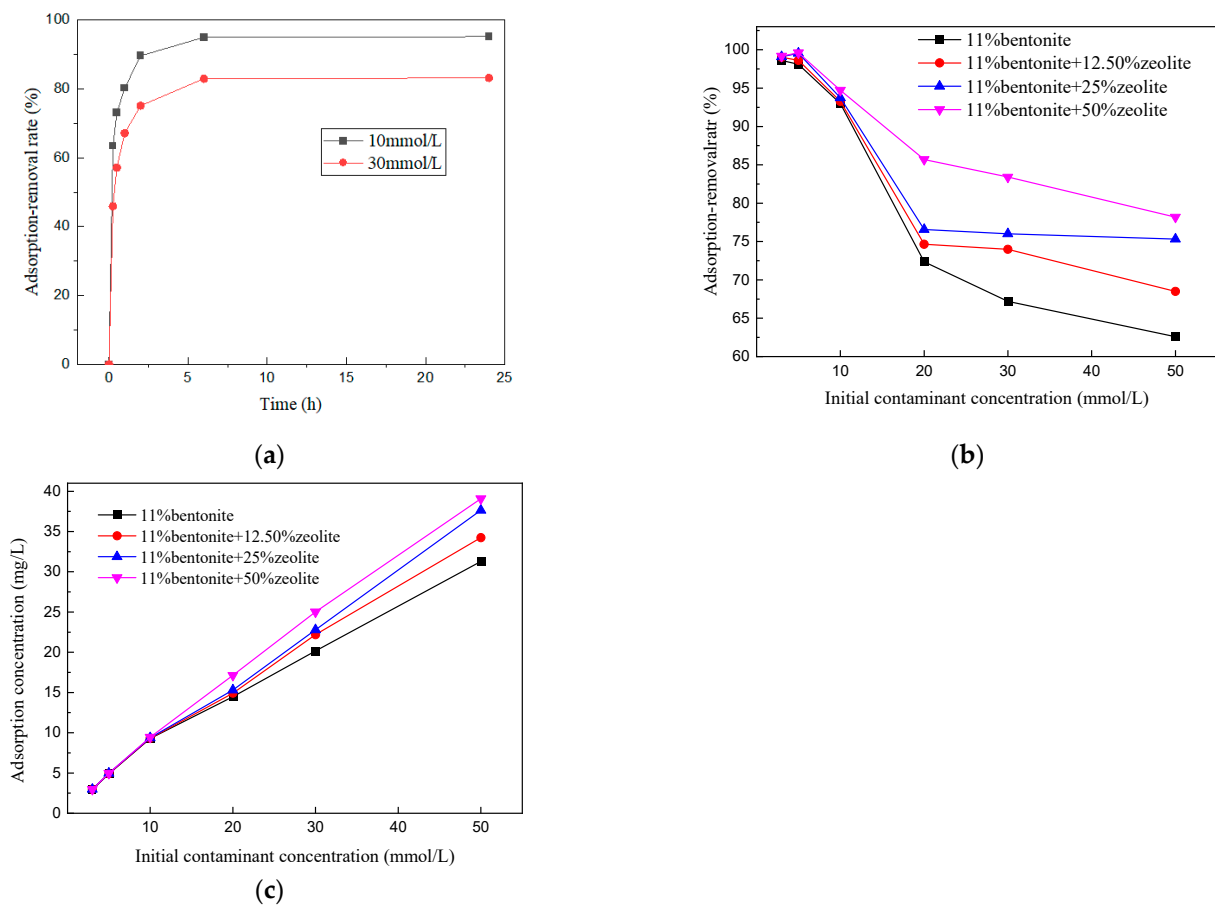


**Figure 8.** ZnCl<sub>2</sub> concentration stone chip-bentonite-zeolite mixture zeolite dopants simultaneously varied the stone chip-bentonite-zeolite mixture sorption and removal rates. (a) removal rate vs. adsorption time; (b) removal rate vs. solution concentration; (c) adsorption concentration.

## (2) Mixed earth ion adsorption rate

Figure 8b shows the variations in the Zn<sup>2+</sup> adsorption concentration of the soil mixture with the initial contaminant concentration. An increase in the initial contaminant concentration causes an increase in the Zn<sup>2+</sup> adsorption concentration of the soil mixture. For a zeolite content of 0%, the soil mixture had adsorption concentrations of 261.95 and 406.64 mg for initial contaminant concentrations of 30 and 50 mmol/L, respectively. The addition of zeolite produced notable changes in the Zn<sup>2+</sup> adsorption concentration. For a given contaminant concentration, increasing the zeolite content produced an increase in the Zn<sup>2+</sup> adsorption concentration of the soil mixture. For example, for a contaminant concentration of 50 mmol/L, the soil mixture had Zn<sup>2+</sup> adsorption concentrations of 444.99, 489.32, and 508.04 mg for zeolite contents of 12.50, 25, and 50%, respectively, corresponding to increments of 9.53, 20.48, and 27.49%.

## (3) Adsorption model

According to the equation for the adsorption of pollutants by mixed soil for model fitting, where the Langmuir model and Freundlich model fitting correlation coefficient R<sup>2</sup> is closer to 1 compared with Henry and D-R isothermal adsorption models, indicating that the adsorption of Zn<sup>2+</sup> by mixed soil is more consistent with the Langmuir model and Freundlich model, and the fitting curves are shown in Figure 9 (the end of the curves in the figure all reached adsorption equilibrium). As can be seen from the figure, the unit adsorption amounts at different concentrations are consistent with each model. The characteristics of heavy metal Zn<sup>2+</sup> adsorption by mixed soil after zeolite incorporation are still accurately defined by the Langmuir and Freundlich models, where the correlation

coefficient  $R^2$  fitted by the Freundlich model is 0.95, and the empirical constants  $n$  are all greater than 1. Table 1 displays the fitted parameters, and the correlation coefficient  $R^2$  demonstrates this. Moreover, Equation (5) shows that the mixed soil is nonlinear for  $Zn^{2+}$ , and  $1/n$  is less than 1, indicating chemisorption is dominant and produces ionic interchange. The Langmuir-based maximum unit adsorption capacities of the zeolite–bentonite–stone chip mixture for zeolite contents 0, 12.50, 25, and 50% were 145.90, 181.80, 253.60, and 423.40 mg/g, respectively. Other conditions are the same, the adsorption capacity of the stone chip–bentonite–zeolite mixture for  $Zn^{2+}$  increases with the increase of bentonite doping, and the experimental results of this paper show that the adsorption capacity of stone chip–bentonite–zeolite mixture with 50% zeolite doping is the strongest.

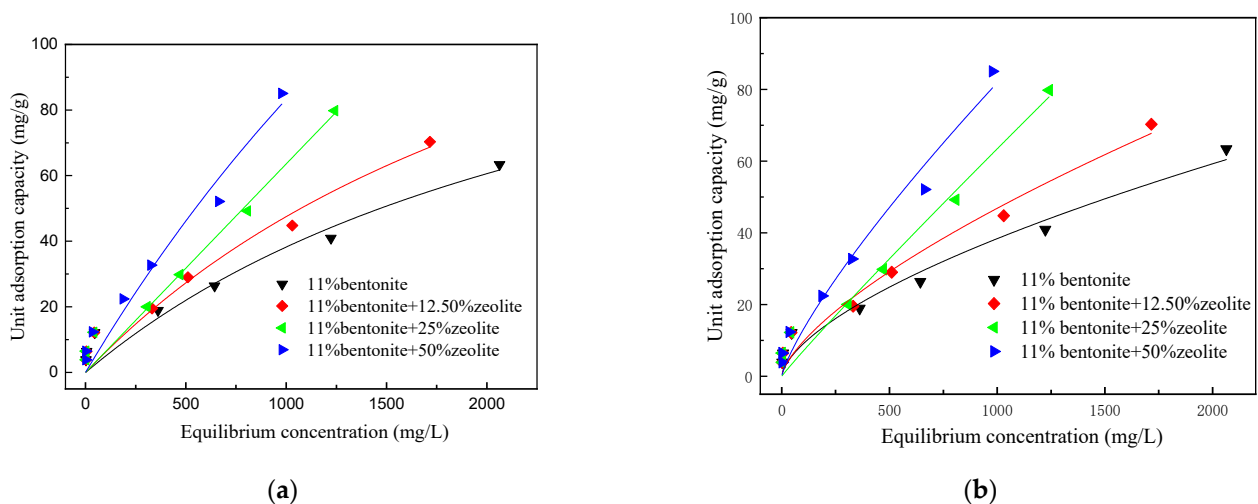


Figure 9. Fitting of adsorption models for mixed soils with simultaneous variations of  $ZnCl_2$  concentration and zeolite dopants. (a) Langmuir model; (b) Freundlich model.

Table 1. Parameters of adsorption model for mixed soils with a simultaneous variation of  $ZnCl_2$  concentration and zeolite dopants.

	Content/ Parameter	Bentonite	Bentonite + 12.50% Zeolite	Bentonite + 25% Zeolite	Bentonite + 50% Zeolite
Langmuir	$K_L$	$3.55 \times 10^{-4}$	$3.54 \times 10^{-4}$	$3.02 \times 10^{-4}$	$2.45 \times 10^{-4}$
	$q_m$	145.90	181.80	253.60	423.40
	$R^2$	0.93	0.94	0.96	0.95
Freundlich	$K_F$	0.51	0.42	0.39	0.33
	$n$	1.60	1.46	1.33	1.25
	$R^2$	0.96	0.96	0.96	0.96

#### 4. Micromechanics

##### 4.1. Influence of Zeolite Doping on the Permeation of Bentonite-Based Liners

###### (1) XRD

From the adsorption test protocol for XRD tests, three samples were chosen. Figure 10 displays the XRD patterns under various test conditions. Under the condition of no zeolite, the intensity of the characteristic diffraction peak of montmorillonite decreased with the increase of the initial concentration of contaminants, which indicated that  $Zn^{2+}$  would lead to the decrease of montmorillonite content; and there was a change in diffraction peak, which indicated that the adsorption test of  $Zn^{2+}$  with bentonite produced new substances; according to the Bragg equation  $2 d \sin \theta = n \lambda$ , the change of diffraction angle and the layer spacing also changed, which indicated that the interlayer of sodium-based bentonite  $Na^+$  and  $Zn^{2+}$  underwent ion exchange. The size of the interlayer hydrated cations determines

the spacing between both the montmorillonite layers, and the hydration capacity of metal cations is inversely proportional to their radius and inversely proportional to their charge. It is illustrated that the higher the ion concentration without zeolite admixture, the greater the permeability coefficient of the mixed soil.  $Zn^{2+}$  is absorbed into the body by sodium-based bentonite, and because  $Zn^{2+}$  carries a more significant charge than  $Na^+$ , the layer spacing increases, and the permeability of the bentonite weakens. Zeolite is incorporated, and the addition results in a new diffraction peak that is not the typical peak of zeolite composition, proving that zeolite is added throughout ion exchange. Interchange is generated by the exchangeable cations in the  $Zn^{2+}$  and zeolite solution. This diminishes the amount of  $Zn^{2+}$  ion exchange that takes place in solution with montmorillonite, weakening the detachment between bentonite layers, increasing bentonite expansion, and improving permeability, which is reflected in a reduction in the permeability coefficient of the mixed soil.

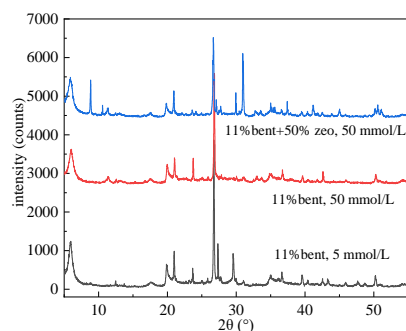


**Figure 10.** Change of XRD.

## (2) SEM

Figure 11 shows a comparison of bentonite SEM images before and after zeolite incorporation under the action of the ionic solution. In a zoomed-in 10K SEM image, it can be seen that the zeolite addition of bentonite as a whole is a large piece of structure with a plume-like morphology, and bentonite indicates the emergence of plume-like colloid exfoliation traces by the solution; bentonite indicates that there is also cracking fragmentation of small particles, producing small flakes of montmorillonite, as shown in Figure 11a. As shown in Figure 11b, in the case of no zeolite, the bentonite produces verified cracking and fragmentation to form small aggregates, the flaky form no longer exists, the pores get bigger and bigger, the swelling performance is weakened, and the permeability coefficient is increased.

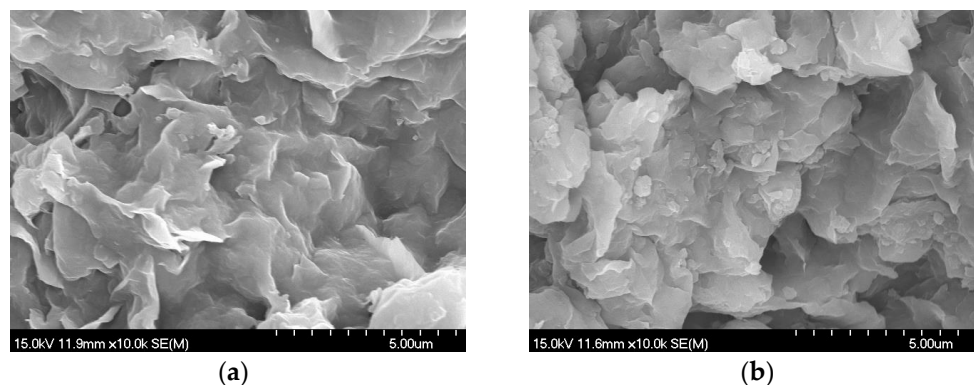


**Figure 11.** The effect of process treatment on material micromorphology. (a) Bentonite SEM image after adding zeolite; (b) Bentonite SEM image without zeolite.

## 4.2. Effect of Zeolite Doping on Metal Adsorption Properties of Mixed Soils

### (1) Zeta potential

Zeta potential value is an essential indicator of the stability of a constant colloidal system, which is judged by measuring the strength of mutual repulsion or attraction between particles. The more stable the particle dispersion system is, the higher the absolute value of zeta potential, while the particle condensation or coalescence is an unstable state.

The results of the potential variation of the stone chip-bentonite-zeolite mixture under different zeolite doping and ion concentration conditions are shown in Figure 12a. The potential of bentonite in pure water was also measured to be  $-39$  mV, and the bentonite particles indicated a negative potential. As can be seen from the Figure, without bentonite doping, in the  $\text{Zn}^{2+}$  solution, the absolute value of the bentonite potential decreases with increasing concentration, such as when the  $\text{Zn}^{2+}$  concentration increases from 10 mmol/L to 50 mmol/L, the potential is  $-11.80$  and  $-7.60$  mV. This is because the exchange of  $\text{Zn}^{2+}$  in solution with the exchangeable cation  $\text{Na}^+$  is indicated by the bentonite particles, making the bentonite double electric layer thickness decrease, resulting in a decrease in the negative charge on the surface of the particles.

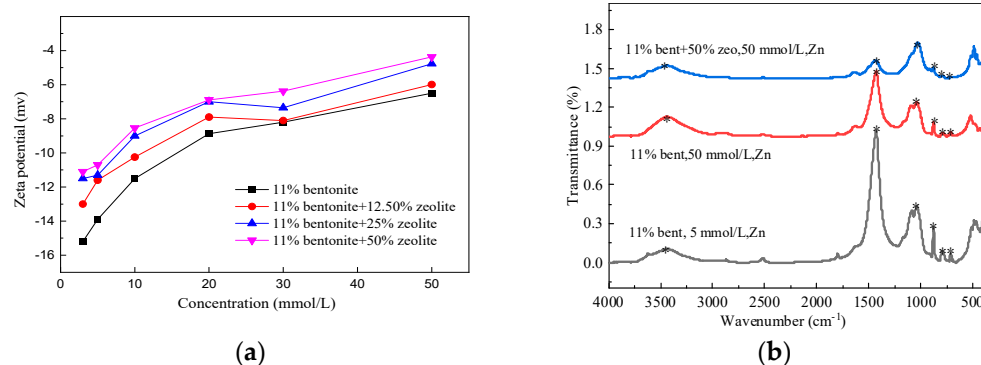


**Figure 12.** Microscopic changes in adsorption tests under different conditions. (a) change of zeta potential; (b) FTIR spectra.

Moreover, as the ionic solution concentration increases, the number of cations near the bentonite particles indicates an increase, and the thickness of the double electric layer is compressed, which shows that the absolute value of zeta potential decreases; the weakening of the negative potential on the surface of the soil particles indicates that the adsorption of  $\text{Zn}^{2+}$  by the mixed soil increases.

When the solution ion concentration is specific, the absolute value of the potential of mixed soil decreases with the increase of zeolite admixture. For example, when the initial concentration of  $\text{Zn}^{2+}$  was 3 mmol/L, the surface potential of bentonite particles was negative, with a potential value of  $-15.20$  mV. After the incorporation of zeolite, the potential of mixed soil samples continued to rise with the increase of zeolite incorporation and was  $-13$ ,  $-11.50$ , and  $-11.10$  mV at 12.50, 25, and 50% incorporation, respectively. With solid adsorption capacity, zeolite added to bentonite will share part of the negative effect of pollutants on bentonite and weaken the compression effect of metal ions on the double bentonite layer. Therefore, under the same concentration conditions, the increase of zeolite doping increases the stone chip-bentonite-zeolite mixture's overall adsorption capacity, as shown by the absolute value of the potential on the surface of the stone chip-bentonite-zeolite mixture decreases with the increase of zeolite doping.

### (2) FTIR spectra

The infrared spectrum analysis of adsorbed different concentrations of  $\text{Zn}^{2+}$  bentonite is shown in Figure 12b. The bentonite layers between the scanning range of  $4000\text{ cm}^{-1}$  and  $400\text{ cm}^{-1}$  and the elastic vibration of the water molecule H-O-H corresponds to a peak at  $3450\text{ cm}^{-1}$ . The peak near  $1425\text{ cm}^{-1}$  corresponds to the unique vibration of the

Si-O-Si bond. As a whole, the basic frame of bentonite remains unchanged before and after adsorption, and the absorption peak changes the same, indicating that heavy metal ions enter the interlayer after adsorption. When the concentration of  $Zn^{2+}$  increases, the peak intensity of the M Al-OH (M metal cation) shock peak at  $877\text{ cm}^{-1}$  decreases, which means that ion exchange has occurred between bentonite and  $Zn^{2+}$ . The aforementioned modifications become more pronounced with the addition of zeolite, indicating that zeolite increases interlayer adsorption and ion exchange to a greater extent.

### (3) Comparison of zeolite-bentonite adsorption properties

The  $Al^{3+}$  in the montmorillonite structure of bentonite is often replaced by other ions of low valence, making the cells appear to have an excess negative charge that can attract other cations. As a consequence, it is regularly used as a metal adsorbent. When zeolite is incorporated, the adsorption capacity of mixed clays is much higher than that when bentonite is used alone.

Compared to biochar, clay minerals, and nanostructured materials, zeolites are widely used because of their environmental friendliness, stability, and low cost. Zeolite-bentonite mixture demonstrated higher  $Zn^{2+}$  removal efficiency compared to bentonite, zeolite, and zeolite-bentonite mixture. Cao et al. [22] manufactured bentonite-zeolite (BZ) adsorbent with bentonite, aluminate, and rice husk. They found that the adsorption capacity of bentonite-zeolite adsorbent for  $Cu^{2+}$  and  $Zn^{2+}$  was improved dramatically, which was in connection with our results. It indicates that zeolite-bentonite hybrid clay has good adsorption performance and can be used as impermeable material for landfill.

## 5. Conclusions

(1) Zeolite can significantly increase the permeability and adsorption capabilities of the stone chip-bentonite-zeolite mixture. The permeability coefficient was reduced from  $10^{-7}\text{ cm/s}$  to  $10^{-8}\text{ cm/s}$  by incorporating 12.50% zeolite. XRD results showed that without zeolite incorporation, ion exchange occurred between sodium-based bentonite and  $Zn^{2+}$ , which increased the layer spacing and reduced the impermeability performance. The addition of zeolite also adsorbed  $Zn^{2+}$  for ion exchange, which reduced the ion exchange of sodium-based bentonite and weakened the increase of layer spacing, as shown by the amount of bentonite swelling increasing, thus increasing the permeability performance of the mixed soil.

(2) Zeolite has a high specific surface area, which contributes to its high adsorption capacity. As zeolite is added to bentonite, it will share a portion of the negative effects of pollutants on bentonite, enhancing the overall adsorption capacity of the mixed soil. At the same concentration, the absolute value of zeta potential falls as zeolite admixture increases.

(3) The Langmuir model and the Freundlich model can be used to describe the isothermal adsorption characteristics of  $Zn^{2+}$  by zeolite doping mixture; according to the Langmuir model, the maximum adsorption number of pollutants adsorbed by the mixture at different zeolite doping can be predicted; according to the Freundlich model, the adsorption is mainly chemisorption, and ionic interchange occurs.

**Author Contributions:** Conceptualization, S.X., Y.F., X.X. and Z.W.; software, Y.F., J.W., J.L. and W.W.; validation, Y.F., W.W. and J.W.; formal analysis, Y.F., J.W. and J.L.; investigation, Y.F., J.W. and J.L.; resources, S.X., X.X. and Z.W.; data curation, W.W., J.W. and Y.F.; writing—original draft preparation, Y.F., S.X. and X.X.; supervision, S.X., X.X. and Z.W. All authors have read and agreed to the published version of the manuscript.

**Funding:** This project was supported by the Zhejiang Provincial Natural Science Foundation (LY20E080022), and the National Natural Science Foundation (52178363, 5207867).

**Data Availability Statement:** Data sharing is not applicable.

**Conflicts of Interest:** The authors declare no conflict of interest.

## References

1. Huang, X.; Li, J.S.; Xue, Q.; Chen, Z.; Du, Y.J.; Wan, Y.; Liu, L.; Poon, C.S. Use of self-hardening slurry for trench cutoff wall: A review. *Constr. Build. Mater.* **2021**, *286*, 122959. [[CrossRef](#)]
2. Narani, S.S.; Abbaspour, M.; Mir Mohammad Hosseini, S.M.; Aflaki, E.; Moghadas, F. Sustainable reuse of Waste Tire Textile Fibers (WTTFs) as reinforcement materials for expansive soils: With a special focus on landfill liners/covers. *J. Clean. Prod.* **2020**, *247*, 119151. [[CrossRef](#)]
3. Ye, W.M.; Chen, Y.G.; Chen, B.; Wang, Q.; Wang, J. Advances on the knowledge of the buffer/backfill properties of heavily-compacted GMZ bentonite. *Eng. Geol.* **2010**, *116*, 12–20. [[CrossRef](#)]
4. Mukherjee, K.; Mishra, A.K. Evaluation of Hydraulic and Strength Characteristics of Sand-Bentonite Mixtures with Added Tire Fiber for Landfill Application. *J. Environ. Eng.* **2019**, *145*, 04019026. [[CrossRef](#)]
5. Otoko, G.R.; Otoko, G.U. The Permeability of Ocean Sand with Bentonite. *Int. J. Eng. Technol. Res.* **2014**, *2*, 1–6. Available online: <https://www.researchgate.net/publication/266200763> (accessed on 15 November 2022).
6. Pawar, R.R.; Lalmunsiama; Bajaj, H.C.; Lee, S.M. Activated bentonite as a low-cost adsorbent for the removal of Cu (II) and Pb (II) from aqueous solutions: Batch and column studies. *J. Ind. Eng. Chem.* **2016**, *34*, 213–223. [[CrossRef](#)]
7. Komine, H. Simplified evaluation for swelling characteristics of bentonites. *Eng. Geol.* **2004**, *71*, 265–279. [[CrossRef](#)]
8. Anirudhan, T.S.; Ramachandran, M. Adsorptive removal of basic dyes from aqueous solutions by surfactant modified bentonite clay (organoclay): Kinetic and competitive adsorption isotherm. *Process Saf. Environ. Prot.* **2015**, *95*, 215–225. [[CrossRef](#)]
9. Kaya, A.; Ören, A.H. Adsorption of zinc from aqueous solutions to bentonite. *J. Hazard. Mater.* **2005**, *125*, 183–189. [[CrossRef](#)]
10. Liu, Z.R.; Zhou, S.Q. Adsorption of copper and nickel on Na-bentonite. *Process Saf. Environ. Prot.* **2010**, *88*, 62–66. [[CrossRef](#)]
11. Yu, K.; Xu, J.; Jiang, X.; Liu, C.; McCall, W.; Lu, J.L. Stabilization of heavy metals in soil using two organo-bentonites. *Chemosphere.* **2017**, *184*, 884–891. [[CrossRef](#)] [[PubMed](#)]
12. Yu, C.; Yang, Y.; Wu, Z.X.; Jiang, J.F.; Liao, R.P.; Deng, Y.F. Experimental study on the permeability and self-healing capacity of geosynthetic clay liners in heavy metal solutions. *Geotext. Geomembr.* **2021**, *49*, 413–419. [[CrossRef](#)]
13. Dutta, J.; Mishra, A.K. Influence of the presence of heavy metals on the behaviour of bentonites. *Environ. Earth Sci.* **2016**, *75*, 993. [[CrossRef](#)]
14. Xu, C.; Liao, X.Y.; Li, Z.B. Influence of Solution Characteristics on Swelling and Hydraulic Performance of Geosynthetic Clay Liners. *Geosynth. Civ. Environ. Eng.* **2009**, 58–63. [[CrossRef](#)]
15. Cabrera, C.; Gabaldón, C.; Marzak, P. Sorption characteristics of heavy metal ions by a natural zeolite. *J. Chem. Technol. Biot.* **2005**, *80*, 477–481. [[CrossRef](#)]
16. Abollino, O.; Aceto, M.; Malandrino, M.; Sarzanini, C.; Mentasti, E. Adsorption of heavy metals on Na-montmorillonite. Effect of pH and organic substances. *Water Res.* **2003**, *37*, 1619–1627. [[CrossRef](#)]
17. Iskander, A.L.; Khald, E.M.; Sheta, A.S. Zinc and manganese sorption behavior by natural zeolite and bentonite. *Ann. Agric. Sci.* **2011**, *56*, 43–48. [[CrossRef](#)]
18. Salem, A.; Akbari, S.R. Removal of lead from solution by combination of natural zeolite–kaolin–bentonite as a new low-cost adsorbent. *Chem. Eng. J.* **2011**, *174*, 619–628. [[CrossRef](#)]
19. Sen, T.K.; Gomez, D. Adsorption of zinc (Zn<sup>2+</sup>) from aqueous solution on natural bentonite. *Desalination* **2011**, *267*, 286–294. [[CrossRef](#)]
20. Badollop-Almaraz, V.; Trocellier, P.; Dávila-Rangel, I. Adsorption of aqueous Zn(II) species on synthetic zeolites. *Nucl. Instrum. Methods B* **2003**, *210*, 424–428. [[CrossRef](#)]
21. Amutenya, E.L.M.; Zhou, F.S.; Liu, J.L.; Long, W.J.; Ma, L.; Liu, M.; Lv, G.M. Preparation of humic acid-bentonite polymer composite: A heavy metal ion adsorbent. *Heliyon* **2022**, *8*, e09720. [[CrossRef](#)] [[PubMed](#)]
22. Cao, L.P.; Li, Z.H.; Xiang, S.Y.; Huang, Z.H.; Roger, R.; Liu, Y.H. Preparation and characteristics of bentonite–zeolite adsorbent and its application in swine wastewater. *Bioresour. Technol.* **2019**, *284*, 448–455. [[CrossRef](#)] [[PubMed](#)]